



Cite this: *RSC Adv.*, 2025, **15**, 4628

Enhanced recovery of rare earth elements from carbonatite ore by biological pretreatment

Bayarbayasgalan Bayarsaikhan,^{1D}^a Altangerel Amarsanaa,^{1D}^a Purevjargal Daramjav,^a Sukhbaatar Batchuluun,^a Lkhagvasuren Damdindorj,^b Ni He,^c Hongbo Zhao^c and Sarangerel Davaasambuu ^{1D}^{a*}

The increasing demand for rare earth elements (REEs) necessitates the development of more efficient and environmentally friendly leaching methods. This study investigates the use of biological pretreatment to improve metal recovery from REE ore obtained from the Mushgia Khudag deposit. Characterization of the ore revealed a total REE content of 6.99%, with X-ray diffraction analysis identifying calcite and apatite as the dominant minerals, while REEs were primarily found in the forms of monazite and parisite. Experimental results demonstrated that ore pre-treated with a mixed thiobacteria culture (Tmix) achieved a 1.40-fold increase in metal recovery compared to direct acid leaching. Additionally, *Bacillus* sp. (*B.* sp.) bacteria improved recovery by 1.07-fold. Monitoring changes in pH, oxidation-reduction potential (ORP), and zeta potential during the pre-treatment process indicated that the bacteria did not directly dissolve the REEs but rather modified the surface charge and mineral structure of the ore, facilitating more efficient acid leaching. The use of Tmix bacteria for pretreatment significantly improved leaching efficiency, reduced acid consumption, and minimized environmental impact.

Received 4th November 2024
 Accepted 27th January 2025

DOI: 10.1039/d4ra07845d
rsc.li/rsc-advances

1. Introduction

In recent years, rare earth elements (REEs) have gained significant attention owing to their critical role in renewable energy technologies, electrical devices, and nuclear applications. Naturally, REEs occur in various forms, with monazite (20%), bastnasite (70%), ion-exchange clays (7%), xenotime (2%), and other forms (1%) by weight.¹ Among these, REE ores derived from monazite are particularly rich in light rare earth elements such as La, Ce, Pr, and Nd.²⁻⁴ Monazite, a phosphate mineral with the composition (Ce, La, Nd, Th)PO₄, has a crystalline structure that imparts high thermal stability, making it challenging to leach. Consequently, leaching and extracting these elements typically require strong acids or alkalis under controlled conditions.⁵⁻⁷ Commonly employed acids in acid leaching systems for REEs containing monazite include hydrochloric acid,^{8,9} phosphoric acid,¹⁰ nitric acid,^{11,12} and sulfuric acid.^{7,13,14} Under ambient conditions, the metal recovery of monazite-containing ores through acid leaching usually ranges from 30% to 70%.^{15,16} However, this recovery can significantly increase to as much as 98% at elevated temperatures.^{2,7} For example, Harry Watts *et al.* achieved a total rare

earth element (TREE) recovery of 95.2% by leaching monazite sands with concentrated (85%) phosphoric acid at high temperatures of 260 °C.¹⁰ Similarly, using 98% sulfuric acid, Helaly *et al.* studied monazite leaching in a temperature range of 160–300 °C and achieved a maximum metal recovery of 93.7% at 220 °C.¹³ Additionally, Panda *et al.* conducted a two-step leaching process with diluted HCl, followed by 6 N HCl on Korean monazite, achieving a metal recovery increase of 3.6 times.⁸ Kuzmin *et al.* also demonstrated a TREE recovery of 97.4% by leaching Chuktukon ore containing monazite with 6 M nitric acid at 200 °C for 2 hours.¹¹

Despite the high efficiency of REE leaching through acid methods, these processes are energy-intensive and generate toxic gases and liquid phases that require further neutralization.

To address these challenges, implementing pretreatment processes that facilitate leaching under milder conditions presents a potential solution.¹⁷ However, research into the pretreatment of monazite ores remains limited. For instance, Mei Li *et al.* roasted a mixed rare earth concentrate (53.59% bastnasite-rare earth oxide and 8.75% monazite-rare earth oxide) with sodium hydroxide at 550 °C for one hour, followed by leaching with 6 M hydrochloric acid at 90 °C, achieving a metal recovery of 92.6%.¹⁸ Although activation methods show promise, they still require high temperatures, extensive chemical use, significant energy consumption, and may have negative environmental impacts. Therefore, finding ways to enhance the efficiency under mild or ambient conditions remains a considerable challenge.

^aDepartment of Chemistry, School of Arts and Sciences, National University of Mongolia, Ulaanbaatar, 14201, Mongolia. E-mail: sarangerel@num.edu.mn

^bDepartment of Biology, School of Arts and Sciences, National University of Mongolia, Ulaanbaatar, 14201, Mongolia

^cSchool of Minerals Processing and Bioengineering, Central South University, Changsha, 410083, China



Recently, there has been growing interest in bioleaching, an environmentally friendly, low-cost, and sustainable technology, as a viable method for leaching REEs under ambient conditions.^{3,19,20} Several studies have explored this approach. For instance, Fathollahzadeh *et al.* used *Enterobacter (E.) aerogenes* and *Acidithiobacillus (A.) ferrooxidans* bacteria to leach REE-rich monazite and florencite minerals at 30 °C and 120 rpm over 12 days. They observed a continuous increase in REE leaching over time, with significant enhancements in the presence of both bacteria due to synergistic effects. It was suggested that *E. aerogenes*, which is known to be tolerant of acidic conditions and capable of producing organic acids, positively influenced the leaching environment created by *A. ferrooxidans*.²¹ Additionally, Corbett *et al.* investigated the impact of carbon sources on bioleaching using *Klebsiella (K.) aerogenes*, *Burkholderia* T48, *Pseudomonas (P.) putida*, and *Gluconobacter (G.) oxydans* on high-grade monazite ore. Their findings revealed that fructose significantly enhanced the leaching efficiency when used with *K. aerogenes* and *Burkholderia* T48, while *P. putida* and *G. oxydans* were more effective with galactose.²⁰

Furthermore, Fathollahzadeh *et al.* examined the indirect mechanisms of bioleaching, focusing on bacterial interactions. Their study showed that organic acids produced as by-products of bacterial metabolism played a crucial role in dissolving REEs.²¹

Overall, the bioleaching of rare earth elements is an environmentally friendly method that operates under milder conditions compared to traditional acid leaching. While it generally requires a longer duration and results in relatively lower recovery, incorporating bacteria in the pretreatment phase can significantly enhance the leaching efficiency. This biological approach can aid in the effective release of rare earth elements from ores, making the process more sustainable and efficient. Building upon these findings, this research aimed to isolate bacterial cultures from natural ores and apply bio-pretreatment under standard conditions to enhance the REE recovery from monazite-containing ores. In this study, REE ore from the Mushgia Khudag deposit was treated with bacterial cultures at room temperature for 7 days. Following bacterial treatment, the ore was filtered, dried, and subjected to acid leaching, which resulted in a total metal recovery increase of 1.4 times compared to the untreated ore.

2. Experimental section

2.1 Sample preparation

2.1.1 Ore sample. The REE ore used in this experiment was collected from the Mushgia Khudag deposit, located in Tsogt-Ovoo soum, Ömnögovi province, Mongolia (coordinates: 44.389676, 103.999740). The ore was initially crushed to <12.5 mm and then ground to <0.074 mm for the leaching experiments.

2.1.2 Bacterial culture. For the bioleaching of REEs, a mixed thiobacteria culture (Tmix) containing *Thiobacillus denitrificans* (GenBank: OR053813.1) and *Bacillus cereus* (GenBank: OR053804.1) was used. We cultivated these bacteria in 9 K nutrient medium, following the protocol of Hong and

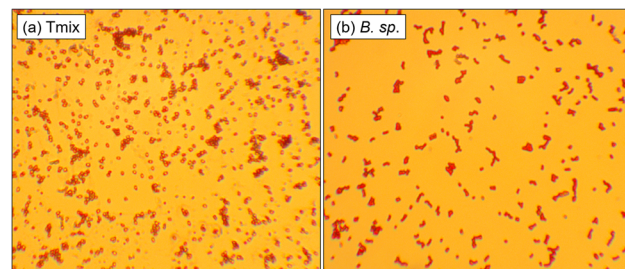


Fig. 1 Optical images of the bacterial cultures: (a) Tmix, (b) *B. sp.*

Silverman.^{22,23} The Tmix culture was originally isolated from high-grade chalcopyrite copper ore. Additionally, a *Bacillus species* (GenBank: 4TH0UUSC016) cultured in NBRIP medium^{24,25} was employed in the experiments. This *Bacillus* strain (*B. sp.*) was isolated from the Mushgia Khudag ore through colony separation on a solid medium from a mixed bacterial culture grown in NBRIP medium. The bacterial cultures used in the bioleaching experiments were stained following the bacterial cell wall staining method.²⁶ The stained bacterial preparations were observed under an optical microscope (BEL Photonics, BEL Engineering) at 400 \times magnification, and microscopic images were captured and are displayed in Fig. 1.

Based on the optical microscope images and the staining of the cell walls, it was observed that Gram-negative, short rod-shaped bacteria predominated in the mixed thiobacteria. *T. denitrificans* is Gram-negative and rod-shaped, while *B. cereus* is Gram-positive and short rod-shaped (Fig. 1a). On the other hand, the *B. sp.* bacteria appeared to be Gram-negative and short rod-shaped. The bacterial populations for bioleaching were quantified through colony counting on a solid medium, revealing that the mixed thiobacteria culture contained 2.1×10^6 CFU mL $^{-1}$, and the *B. sp.* culture contained 4.7×10^6 CFU mL $^{-1}$, both of which were deemed suitable for use in the bioleaching experiments.^{20,27}

2.1.3 Leaching experiments. A total of 40.0 g of REE ore from the Mushgia Khudag deposit was weighed and placed in a 250 mL Erlenmeyer flask along with 80 mL of the bacterial cultures from Tmix and *B. sp.* The bio-pretreatment was carried out at 30 °C with shaking at 200 rpm for 7 days. After that, the solid and liquid phases were separated, and the solid residue was rinsed twice with distilled water and then dried at 60 °C for subsequent acid leaching and X-ray diffraction (XRD) analysis. Acid leaching of the bio-pretreated REE ore residue was performed using 1.0 M H₂SO₄ under previously established conditions,²⁸ with a solid-to-liquid ratio of 1:6, agitation at 200 rpm, and a temperature of 30 °C for 20 h. During the leaching, the pH of the solution was measured using a pH meter (Hi2211, Hanna), and the oxidation-reduction potential (ORP) was monitored using platinum and silver chloride electrodes with a pH/ORP meter (Hi9017, Hanna). All the experiments were conducted in duplicate to ensure reliability. The standard deviation of the results was calculated using standard statistical methods for sampling analysis.



The concentration of REEs in the leachate was determined by inductively coupled plasma optical emission spectrometry (ICP-OES, ICAP 7400, Thermo Fisher Scientific). Metal recovery was then calculated using eqn (1).

$$\varepsilon = \left(\frac{C_{\text{Me}} \times d \times V}{m_{\text{ore}} \times C_{\text{Me,ore}}} \right) \times 100\% \quad (1)$$

where ε represents the metal recovery (%), C is the metal concentration in the leachate (mg L^{-1}), d is the dilution factor, V is the volume (L), m_{ore} is the mass of the initial ore (g), and $C_{\text{Me,ore}}$ is the metal concentration in the ore (mg kg^{-1}).

2.2 Characterization

2.2.1 Chemical analysis. For the chemical analysis of the initial sample, 0.5000 g of ore was accurately weighed and dissolved in a mixture of four acids: hydrochloric acid (HCl), nitric acid (HNO_3), perchloric acid (HClO_4), and hydrofluoric acid (HF). The elemental composition was analyzed using ICP-OES. All reagents used were of analytical grade, and were obtained from UnionLab Co. Ltd (Shanghai, China). To determine the concentration of REEs, a combined method of alkali fusion and acid digestion was applied to chemically process the sample for analysis.

2.2.2 X-ray diffraction analysis. XRD patterns of the initial ore sample and the solid residues after leaching were obtained using a Maxima X7000 X-ray diffractometer (Shimadzu) equipped with a Co $\text{K}\alpha$ radiation source ($\lambda = 0.1793 \text{ nm}$) at a step size of 0.05° . Phase analysis was performed using the Match! software, which identified and characterized the XRD patterns by comparing them with data from the International Centre for Diffraction Data (ICDD) and the RRUFF database.

2.2.3 Fourier transformed infrared analysis. The infrared spectra of the samples were obtained using a Fourier transformed infrared (FTIR) spectrometer (IR Prestige-21, Shimadzu). The sample was prepared at a ratio of 1 : 100 solid residual and KBr (UnionLab, purity $\geq 99.99\%$), and the transmittance was measured in the wavenumber range of $400\text{--}4000 \text{ cm}^{-1}$.

2.2.4 Zeta potential analysis. Zeta potential measurements were performed on three solutions, namely a stock bacterial cultural solution, and the supernatant solutions following bacterial pretreatment and acid leaching. Prior to measurement, each solution was filtered through $125 \mu\text{m}$ pore-size filter paper to remove any particulate matter. The zeta potential was then determined using a zeta potential and particle-size analyzer (ZEECOM ZC-3000, Microtec Co.). This instrument dynamically measured the intensity of scattered light using a CCD camera, and the obtained data was then used to calculate the electrokinetic mobility, which then yielded the zeta potential.

3. Results and discussion

3.1 Chemical and phase analysis of the raw material

Geological investigations have confirmed that the economically significant ore minerals at the Mushgia Khudag deposit include parisite, calcite, apatite, phosphate, and monazite. These minerals are associated with ore bodies composed of

Table 1 Chemical composition of the Mushgia Khudag ore

Content, wt%

SiO_2	Al_2O_3	CaO	MgO	TiFe_2O_3	TiO_2	K_2O	Na_2O	MnO	P_2O_5
21.28	1.74	26.21	0.46	10.98	0.22	0.66	0.45	0.25	14.61
LOI*	CO_2	SO_3	Sr	La	Ce	Pr	Nd	Sm	Y
8.96	6.23	6.39	2.53	2.32	2.84	0.67	0.87	0.09	0.08

Content, mg kg⁻¹

As	Ba	Cd	Co	Cr	Cu	Ga	Gd	Ni
130.34	306.34	1.65	14.00	18.15	76.97	107.14	250.91	32.75
Be	Bi	V	Zn	Zr	Yb	Lu	Se	Ta
9.50	63.80	153.88	425.53	116.23	43.31	7.32	71.80	120.27
Tb	Mo	Nb	Er	Dy	Eu	Li	Pb	Te
43.77	68.38	75.56	132.68	542.60	129.54	51.34	274.21	161.65

phosphate–carbonate, sulfate–silicate–carbonate, carbonate, and quartz–fluorite–carbonate veins and lenses.^{29,30}

A comprehensive understanding of the leaching behaviour of REE ores requires detailed knowledge of the chemical composition and mineral phases present in the initial sample. The chemical composition of the Mushgia Khudag ore analysed in this study is provided in Table 1.

The initial sample was characterized by high concentrations of SiO_2 , CaO , P_2O_5 , and TiFe_2O_3 , each exceeding 10%. In contrast, Sr, CO_2 , and SO_3 were present in moderate amounts, ranging from 2.5% to 6.4%. The ore's economic significance stems from a notable concentration of light REEs, especially lanthanum (La) and cerium (Ce), accompanied by significant amounts of praseodymium (Pr), neodymium (Nd), yttrium (Y), and samarium (Sm). These elements are critical to various high-tech industries, including light emitting diodes, lasers, electric vehicles, and NiMH batteries, making efficient REE extraction from this ore strategically and economically valuable.

The total REE content was 6.99%, classifying the Mushgia Khudag ore as light REE-rich, consistent with previous studies.³¹

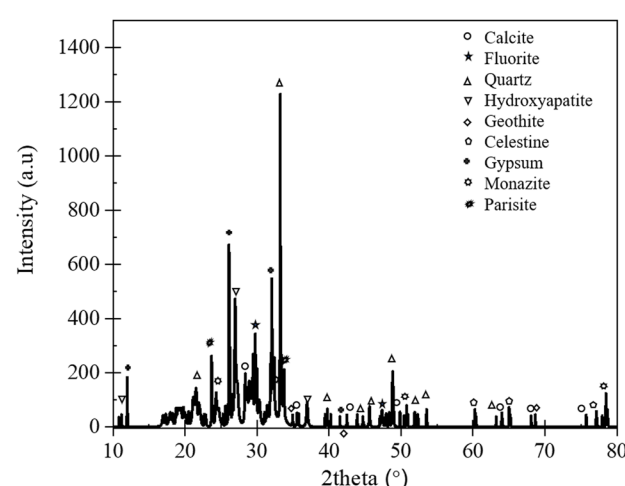


Fig. 2 X-ray diffraction pattern of the ore sample from the Mushgia Khudag deposit.



To further correlate the chemical composition with the corresponding mineral phases, X-ray diffraction analysis was performed. The results of the analysis are presented in Fig. 2.

Consistent with the chemical analysis (Table 1), the Mushgia Khudag ore contained minerals such as quartz (SiO_2), hydroxyapatite ($\text{Ca}_5(\text{PO}_4)_3\text{OH}$), calcite (CaCO_3), gypsum ($\text{CaSO}_4 \cdot 2\text{H}_2\text{O}$), fluorite (CaF_2), goethite (FeOOH), and celestine (SrSO_4). XRD analysis further revealed peaks corresponding to REE-bearing minerals, including monazite ($(\text{La}, \text{Ce}, \text{Nd})\text{PO}_4$) and parisite ($\text{Ca}(\text{Ce}, \text{La})_2(\text{CO}_3)_3\text{F}_2$). These findings align with the observations of Jargalan,³⁰ who reported that monazite, the primary REE-bearing mineral, occurs in association with apatite, often filling the spaces between apatite grains or along fractures within the apatite structure.

3.2 Combined acid and bacterial leaching

The bioleaching was conducted over 7 days using *B. sp.*, isolated from the Mushgia Khudag ore, and Tmix bacteria, derived from high-grade chalcopyrite copper ore. After the bioleaching step, sequential acid leaching was performed to compare the efficiency of both leaching processes (Fig. 3). This study showed how bacterial pretreatment improved the subsequent acid leaching. Bioleaching significantly enhanced REE recovery from the Mushgia Khudag ore. The bioleaching of REE ore using the *B. sp.* and Tmix bacteria resulted in relatively low REE concentrations in the leachate, with recovery rates of merely 0.003% (1.12 mg L^{-1}) and 2.4% (838.68 mg L^{-1}), respectively. These findings indicate that the bacteria were not highly effective in directly leaching REEs into the solution. Certain types of bacteria, including *Thiobacteria*,³² *Pseudomonas*,^{33,34} *Mesorhizobium*,³³ *Acetobacter*,³³ *Enterobacter*,^{32,34} *Burkholderia*,^{3,20} *Klebsiella*,²⁰ and *Pantoea*,³⁴ have been investigated for the biol leaching of rare earth elements (REEs) from monazite ore or concentrate. Among these studies, the highest total REE (TREE) recovery recorded was 25.5 mg L^{-1} ,³⁴ while the lowest recovery was 4 mg L^{-1} .³² In comparison to our study, although these values exceed the leaching efficiency obtained with *B. sp.*, it was noteworthy that the TREE recovery associated with Tmix

surpassed that of all the aforementioned studies. This finding suggests that while *B. sp.* may yield lower TREE recovery, the efficiency of Tmix resulted in a higher concentration of TREES, underscoring their potential applicability in bioleaching processes.

However, acid leaching following bacterial pretreatment showed a significant improvement in REE recovery. The total REE recovery after pretreatment with Tmix and *B. sp.* bacteria increased from $3173.44 \text{ mg L}^{-1}$ to $4539.50 \text{ mg L}^{-1}$ and to $3387.97 \text{ mg L}^{-1}$, respectively, compared to REE recovery from direct acid leaching.

These results suggest that, although the bacteria may not directly dissolve REEs, Tmix bacteria, in particular, play a crucial role in pre-treating the ore. This pretreatment likely alters the surface area and surface charge of associated minerals, thereby enhancing the effectiveness of the subsequent acid leaching.³⁵

Fig. 4 presents the individual metal recovery for each REE, comparing the results of acid leaching with and without bacterial pretreatment. The data highlight the significant impact of bacterial pretreatment on enhancing metal recovery, with improved leaching efficiency demonstrated for most REEs following microbial treatment.

In all cases, the use of Tmix bacteria prior to acid leaching led to the most significant improvement in metal recovery. Notably, Ce and Sm demonstrated the greatest enhancements, with recovery rates 1.44 times higher than those obtained from acid leaching alone. The smallest increase with Tmix bacteria, 1.15 times, was observed for Er. In contrast, with the *B. sp.* bacteria, Ce and Sm showed the highest recovery increases of 1.07 times, while Er had the smallest increase at 1.04 times.³⁶

Several studies have explored various approaches to enhance REE recovery through thermal pretreatment followed by acid leaching. For example, Archana reported that roasting monazite (containing 13.5% lanthanum) with KOH at 250°C , followed by leaching with 1.0 M HCl and 10% H_2O_2 at 80°C for 120 min, achieved an 80% TREE leaching efficiency.³⁷ However, while this approach demonstrated high efficiency, it required the use

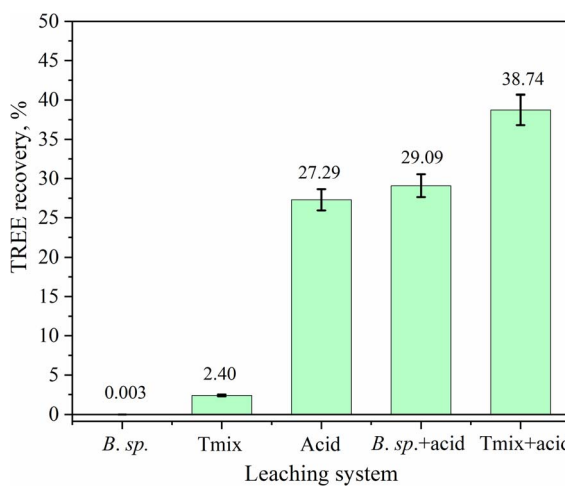


Fig. 3 TREE recovery for the different leaching systems.

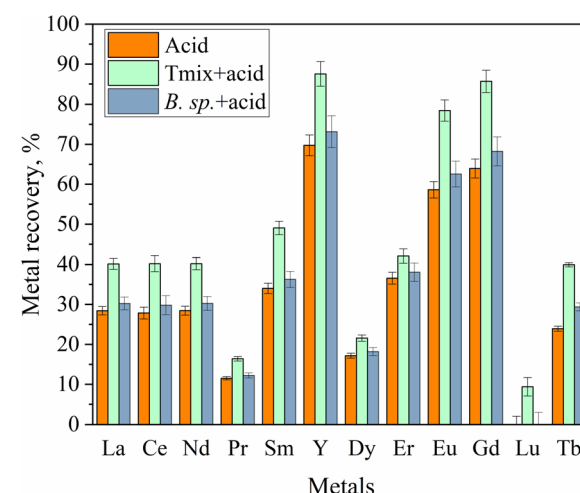


Fig. 4 Metal recovery of REEs with different leaching systems.



of highly concentrated acids and strong oxidizing agents, along with substantial energy consumption and harsh processing conditions, posing environmental and operational challenges.

In contrast, bioleaching and bacterial pretreatment approaches using Tmix and *B. sp.* bacteria offer a more sustainable alternative with the potential to reduce energy consumption and minimize environmental impact. However, further optimization of these biological pretreatment approaches is necessary to improve the leaching efficiency and make them viable for large-scale REE recovery.

3.3 Potential application of bacteria for the pretreatment of acid leaching

The ability of Tmix bacteria to enhance the leaching of REE ores indicates its potential as an effective pretreatment approach prior to acid leaching. To evaluate the feasibility of this approach, it was crucial to monitor several key parameters throughout the leaching process. These included pH fluctuations, changes in ORP and surface charge, and alterations in the mineral composition of the solid phase (Fig. 5).

When the ore was treated with Tmix and *B. sp.* bacteria, the pH of the leachate increased by 4.1 and 0.6, respectively. After subsequent acid leaching, the pH rose further by 0.91 and 0.94. In comparison, when untreated ore was directly subjected to acid leaching, the pH increase was only 0.69.

As the REE ore originates from a carbonatite deposit and contains a high concentration of calcite, the interaction between the carbonate rock and hydroxide ions from the Tmix bacterial solution resulted in a sharp increase in pH. This increase was attributed to the leaching of carbonate minerals under the influence of hydroxide ions, creating favourable conditions for efficient acid leaching. Acid leaching of the ore pretreated with Tmix bacteria resulted in a significantly higher metal recovery compared to that obtained from direct acid leaching (Fig. 3).

An interesting trend was observed regarding the ORP (Fig. 5b). When the ore was treated with bacteria, the ORP decreased initially but then increased during subsequent acid leaching. Typically, the ORP increases when oxidized species dominate the system and decreases in the presence of reduced species. The initial ORP values of the bacterial solutions were 618 mV for Tmix and 441 mV for *B. sp.*

The ORP is influenced by several factors, including the solution's pH, temperature, and chemical species, such as dissolved oxygen. Since the leaching experiments were conducted

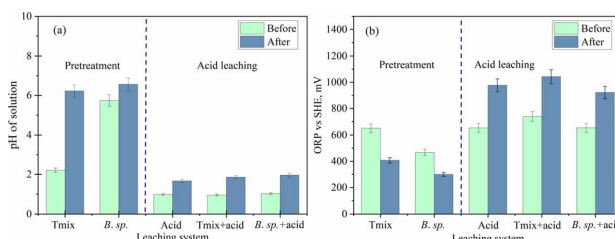
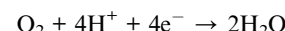


Fig. 5 (a) pH and (b) ORP values for the different pretreatment and acid leaching approaches.

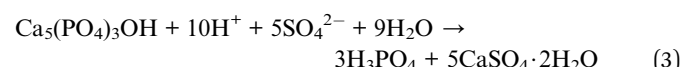
at a constant temperature, the observed increase in ORP during acid treatment of the bacteria-pretreated ore could be attributed to the influence of oxygen in the system, aligning with the following half-reaction:



As no aerobic bacteria were present in the system, this reaction directly reflects the role of oxygen during the acid leaching process. Conversely, when the ore was treated with bacteria, the pH of the solution increased while the ORP decreased. This reduction in ORP was due to the consumption of dissolved oxygen during bacterial respiration. As the bacteria metabolize, the oxygen levels decrease, resulting in a lower ORP value, which, combined with the increase in pH, leads to enhanced leaching conditions.

To further evaluate the effect of bacterial treatment on the mineral phases of the REE-containing rock, XRD analysis was conducted on the solid residue following pretreatment of the Mushgia Khudag ore with Tmix and *B. sp.* bacteria, followed by acid leaching. The results of this analysis are presented in Fig. 6.

The analysis showed that in both cases where the rare earth element oxide was pretreated with bacteria, the intensity of the apatite peak decreased, while the gypsum peak intensity increased following treatment with Tmix bacteria. The increase in the gypsum peak was attributed to the high concentration of sulfate ions (15.2 g L^{-1}) present in the 9 K nutrient medium used for the Tmix bacteria. Gypsum formation was also linked to the release of calcium ions resulting from the leaching of apatite and calcite minerals, as described by eqn (2) and (3).



After acid leaching, peaks corresponding to minerals such as apatite, calcite, and fluorite, which are known to dissolve in acidic conditions, could no longer be detected in the X-ray

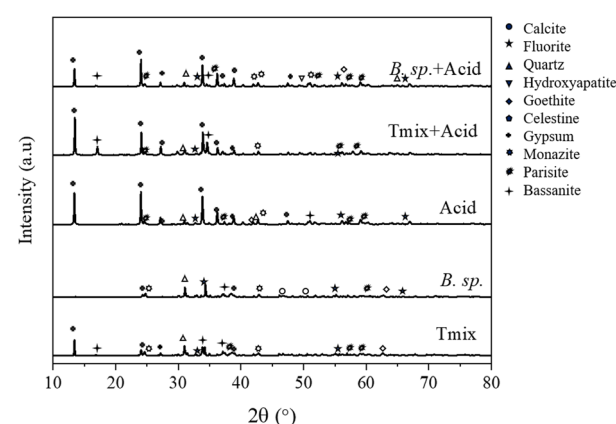
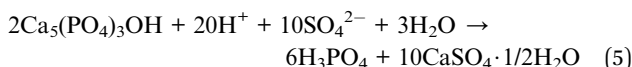


Fig. 6 XRD patterns after bio-pretreatment and acid leaching.



diffractogram. In contrast, the peak intensities of quartz and goethite, which are insoluble in acid, remained unchanged, while the peak intensity of celestine decreased (Fig. 5b). The reduction in celestine's peak intensity was likely not due to its leaching but rather the overlapping of its peaks with those of the newly formed minerals. Meanwhile, the peak intensity of gypsum increased, and the presence of bassanite, a new mineral phase, could be identified, which likely formed during the acid leaching of the REE ore through specific interactions, as described by eqn (4).



The bacterial leachate was acidic, with pH values of 1.6 for Tmix and 4.0 for *B. sp.* However, the system's pH sharply increased due to the leaching of ores rich in calcite, as shown in eqn (2)–(5) (Fig. 5a). Additionally, the decrease in peak intensity of the REE minerals monazite and parisite suggested that the leaching of associated host rocks, such as calcite and apatite, led to a release of REE minerals, thereby enhancing the overall leaching efficiency.

To confirm whether the chemical bonds and compositions changed after bacterial and acid treatment, FTIR spectral analysis was performed, with the results presented in Fig. 7.

The initial analysis of the infrared spectrum revealed the characteristic peaks of calcite³⁸ at 875.68, 1423.47, 1782.23, and 2515.18 cm^{-1} ; however, these peaks disappeared following

bacterial pretreatment. This observation further corroborated the dissolution of calcite mediated by bacterial activity (eqn (2)–(5)). In all cases, except for the initial ore, new peaks corresponding to P–O stretching vibrations at 460 cm^{-1} and P=O stretching vibrations at 601.79 cm^{-1} were identified.³⁹ This change was indicative of the dissolution of apatite in the ore during both the pretreatment and acid leaching processes (eqn (5)), resulting in phosphate ions being adsorbed onto the surfaces of the solid residual particles.

Following the treatment with Tmix and subsequent acid leaching, two weak signals were observed at approximately 601.79 and 667.37 cm^{-1} , as well as at 1118 and 1143 cm^{-1} , which were attributed to the asymmetric stretching vibrations of sulfate.^{40,41} Moreover, the peaks observed around 1622.13–1685.79 and 3408.22–3549.02 cm^{-1} corresponded to the bending and stretching vibrations of water molecules present in gypsum.^{42,43} This observation further validated the formation of gypsum (eqn (2)–(5)), as supported by the XRD analysis results, illustrating the influence of the sulfate ions derived from the Tmix cultural medium and sulfuric acid. The leaching of associated minerals, such as apatite and calcite, through bacterial involvement altered the surface charge of the ore. Therefore, to evaluate the impact of bacterial treatment on the leaching process, the surface charge was measured, with the results presented in Fig. 8.

The particles of the REE ore were negatively charged,²⁸ resulting in a repulsion of similarly charged species or the attraction of oppositely charged species. In parallel, the *B. sp.* bacteria also exhibited a negative charge, while the Tmix bacteria were positively charged (Fig. 8a). As the negatively charged Mushgia Khudag ore interacted with ions and *B. sp.* bacteria, the zeta potential value decreased in both cases (Fig. 8b). This decrease indicated that surface interactions occurred, as corroborated by the XRD and FTIR analysis results.

The attraction of positively charged ions to the negatively charged ore facilitated surface interactions, leading to the formation of smaller, negatively charged particles.⁴⁴ Furthermore, the reduction in particle size was correlated with an increase in the number of negatively charged ore particles,⁴⁵ resulting in a significant decrease in zeta potential. The increase in the number of smaller particles suggested a higher leaching rate.

After acid treatment, the surface charge increased in all cases (Fig. 8c), indicating that the acid interacted with the ore particles, further modifying their surface properties.⁴⁴

The increase in surface potential during acid leaching of the ore treated with Tmix bacteria was greater than that observed

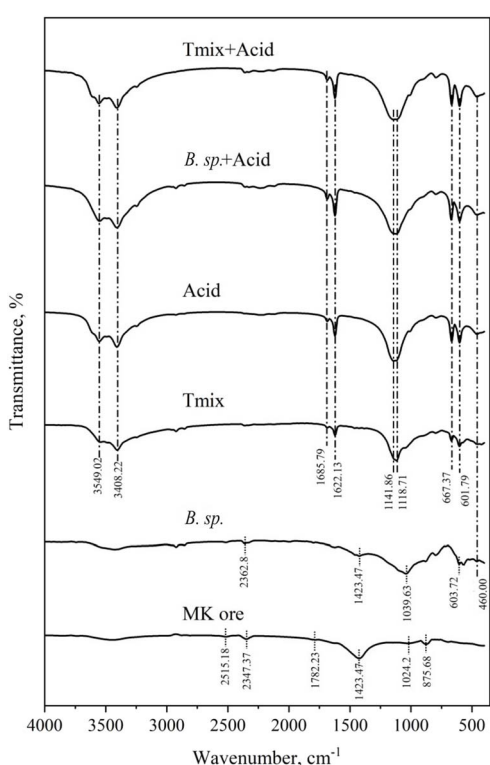


Fig. 7 FTIR spectra after bio-pretreatment and acid leaching.

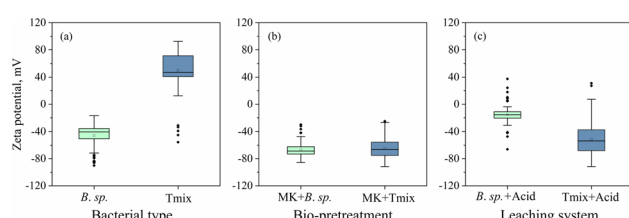


Fig. 8 Changes in surface charge: (a) bacterial culture, (b) after bacterial pretreatment, (c) after acid leaching.



with the *B. sp.* bacteria. The interaction between the strongly positively charged Tmix bacteria and protons led to a significant rise in surface potential. In this case, the amount of dissolved oxygen in the initial leaching solution played a primary role, indicating that the interaction of O_2 and protons predominated over the bacterial count. This finding supports the observation that metal recovery from acid leaching was higher for the ore pretreated with Tmix bacteria compared to ore pretreated with *B. sp.* bacteria (Fig. 3).

This suggests that *B. sp.* bacteria may have primarily facilitated bioactivation through indirect interactions with the Mushgia Khudag ore. In contrast, the Tmix bacteria, due to their positive charge, attracted negatively charged particles, facilitating interactions with the REEs through a cooperative mechanism.⁴⁶ Additionally, hydronium ions produced by *Thiobacillus species*, along with organic acids released as metabolic by-products from *Bacillus species*,^{47–49} played a crucial role in this bioleaching process.⁴⁶ As illustrated in Fig. 5, the bacterial activity throughout the ore treatment was monitored by measuring the pH and ORP. The free protons or hydronium ions derived from *Thiobacillus*, and the organic acids produced by *Bacillus species* interacted with REE ore particles,⁴⁶ leading to the formation of a solution containing anions such as CO_3^{2-} and PO_4^{3-} , as well as cations, including Ca^{2+} and REE^{3+} . These cations tend to form complexes with trace amounts of organic acid residues,^{46,47} while the anions adsorb onto the surfaces of the particles,⁴⁷ resulting in the generation of negatively charged particles. The increased intensity of the PO_4^{3-} bands observed in the infrared spectra aligned with the adsorption of PO_4^{3-} onto the particles, which contributed to their negative charges. As noted in the results regarding the changes in surface charge, the degree of negative charge on the particles treated with Tmix was significantly greater than that observed with the particles treated with *Bacillus species*. This discrepancy could be attributed to the more effective cooperative mechanism employed by Tmix compared to the indirect mechanism utilized by *B. sp.*, thereby enhancing the overall leaching efficiency.

4. Conclusion

This study highlights the significant potential of bio-pretreatment in enhancing the extraction of REEs from monazite ore using Tmix and *B. sp.* bacteria. The results demonstrate that this biological pretreatment approach improved the metal recovery rates by 1.4 and 1.07 times, respectively, compared to acid or biological leaching under ambient conditions. The successful application of microorganisms underscores their capacity to facilitate the leaching of REE-bearing minerals, offering an environmentally friendly alternative to traditional extraction approaches.

The bioleaching process effectively facilitated the dissolution of apatite, the primary mineral in the ore, promoting the release of associated REE minerals. This was confirmed through FTIR and XRD analyses, which also revealed distinct patterns in the pH, ORP, and surface charge. Specifically, the monazite ore exhibited a negative surface charge, while the Tmix bacteria carried a positive charge. These contrasting charges enabled

both direct and indirect interactions that enhanced mineral leaching. In comparison, the *B. sp.* bacteria were limited to indirect interactions, suggesting their suitability for pretreatment purposes.

While these findings are promising, further optimization of the bio-preparation process is necessary to maximize the recovery efficiency. Ongoing research into the underlying mechanisms of bioleaching will provide further valuable insights, and should facilitate the development of sustainable REE extraction methods through the integration of biological and chemical approaches.

Data availability

The original data of the study are included in the article. Further inquiries may be directed to the corresponding authors.

Author contributions

Bayarbayasgalan Bayarsaikhan: investigation, methodology, formal analysis, data curation, resources, writing-original draft. Altangerel Amarsanaa: investigation, methodology, formal analysis, data curation, resources, writing-original draft, visualization data curation, formal analysis, investigation, visualization, methodology. Purevjargal Daramjav: data curation, methodology, validation. Sukhbaatar Batchuluun: data curation, formal analysis, investigation, resources. Lkhagvasuren Damdinordj: investigation, methodology. Ni He: investigation, methodology, formal analysis. Hongbo Zhao: supervision, validation, writing-review & editing. Sarangerel Davaasambuu: conceptualization, data curation, funding acquisition, project administration, supervision, validation, and writing-review and editing.

Conflicts of interest

The authors have no conflicts of interest to declare.

Acknowledgements

This research was supported by the joint project between Mongolian Foundation for Science and Technology and Ministry of Science and Technology of China (CHN-2022/272).

References

- 1 *Industrial Minerals & Rocks*, ed., J. E. Kogel, N. C. Trivedi, J. M. Barker and S. T. Kukowski, Society for Mining, Metallurgy and exploration, Inc, Littleton, 7th edn, 2006.
- 2 I. B. D. Lima and W. Leal Filho, in *Rare Earths Industry*, Elsevier, 2014.
- 3 L. Castro, H. Gómez-Álvarez, M. Carmona, F. González and J. A. Muñoz, *Hydrometallurgy*, 2023, 222, 106178.
- 4 Z. Chen, Z. Han, B. Gao, H. Zhao, G. Qiu and L. Shen, *J. Environ. Manage.*, 2024, 371, 123217.
- 5 A. Shahbaz, *Miner. Eng.*, 2022, 184, 107632.



6 Y. Zhao, X. Sun, D. Meng, X. Liu, Q. Zhong and Z. Feng, *J. Rare Earths*, 2024, **42**, 409–414.

7 J. Demol, E. Ho, K. Sodenhoff and G. Senanayake, *Hydrometallurgy*, 2019, **188**, 123–139.

8 R. Panda, A. Kumari, M. K. Jha, J. Hait, V. Kumar, J. Rajesh Kumar and J. Y. Lee, *J. Ind. Eng. Chem.*, 2014, **20**, 2035–2042.

9 E. H. Borai, M. S. A. El-Ghany, I. M. Ahmed, M. M. Hamed, A. M. S. El-Din and H. F. Aly, *Int. J. Miner. Process.*, 2016, **149**, 34–41.

10 H. Watts and T. Fisher, *Minerals*, 2021, **11**, 1–11.

11 D. V. Kuzmin, N. V. Gudkova, M. N. Leskiv, A. A. Kuzmina and V. I. Kuzmin, *Hydrometallurgy*, 2023, **217**, 106042.

12 E. Jorjani, A. H. Bagherieh and S. C. Chelgani, *Korean J. Chem. Eng.*, 2011, **28**, 557–562.

13 O. Helaly, N. Abdelmonem, K. Abd El-Baky, M. Nogami and I. Ismail, *Water, Energy, Food and Environment Journal*, 2021, **2**, 1–9.

14 J. Demol, E. Ho and G. Senanayake, *Hydrometallurgy*, 2018, **179**, 254–267.

15 G. Wallace, S. Dudley, W. Gleason, C. Young, L. Twidwell, J. Downey, H. Huang, R. James and E. Rosenberg, in *Rare Metal Technology 2015*, Wiley, 2015, vol. 15–19–Marc, pp. 127–134.

16 J. Demol, E. Ho, K. Sodenhoff and G. Senanayake, *Hydrometallurgy*, 2024, **226**, 106296.

17 A. Kumari, R. Panda, M. K. Jha, J. R. Kumar and J. Y. Lee, *Miner. Eng.*, 2015, **79**, 102–115.

18 M. Li, J. Li, D. Zhang, K. Gao, H. Wang, W. Xu, J. Geng, X. Zhang and X. Ma, *J. Rare Earths*, 2020, **38**, 1019–1029.

19 H. Fathollahzadeh, M. J. Hackett, H. N. Khaleque, J. J. Eksteen, A. H. Kaksonen and E. L. J. Watkin, *Bioresour. Technol. Rep.*, 2018, **3**, 109–118.

20 M. K. Corbett, A. Gifford, N. Fimognari and E. L. J. Watkin, *Res. Microbiol.*, 2024, **175**, 104133.

21 H. Fathollahzadeh, T. Becker, J. J. Eksteen, A. H. Kaksonen and E. L. J. Watkin, *Bioresour. Technol. Rep.*, 2018, **3**, 102–108.

22 M. Hong, X. Huang, X. Gan, G. Qiu and J. Wang, *Miner. Eng.*, 2021, **172**, 107145.

23 M. P. Silverman and D. G. Lundgren, *J. Bacteriol.*, 1959, **77**, 642–647.

24 C. S. Nautiyal, *FEMS Microbiol. Lett.*, 1999, **170**, 265–270.

25 P. Delvasto, A. Ballester, J. A. Muñoz, F. González, M. L. Blázquez, J. M. Igual, A. Valverde and C. García-Balboa, *Miner. Eng.*, 2009, **22**, 1–9.

26 J. Harley, *Laboratory Exercise in Microbiology*, McGraw-Hill, 5th edn, 2002.

27 Y. Rodríguez, A. Ballester, M. L. Blázquez, F. González and J. A. Muñoz, *Hydrometallurgy*, 2003, **71**, 57–66.

28 B. Sukhbaatar, D. Purevjargal, S. Tuul, A. Altangerel and D. Sarangerel, *ChemistrySelect*, 2024, **9**, 1–9.

29 J. Dostal and O. Gerel, *Minerals*, 2023, **13**, 129.

30 S. Jargalan, *Rare Earth Metal in Mongolia*, Ulaanbaatar, 1st edn, 2021.

31 B. Munkhtsetseg and G. Burmaa, *Rare Earth Elements in Mongolia*, Nickel Deckel LLC, Ulaanbaatar, 1st edn, 2023.

32 H. Fathollahzadeh, H. N. Khaleque, J. Eksteen, A. H. Kaksonen and E. L. J. Watkin, *Hydrometallurgy*, 2019, **189**, 105137.

33 D. Shin, J. Kim, B. S. Kim, J. Jeong and J. C. Lee, *Minerals*, 2015, **5**, 189–202.

34 M. K. Corbett, J. J. Eksteen, X. Z. Niu and E. L. J. Watkin, *Res. Microbiol.*, 2018, **169**, 558–568.

35 A. Pawlowska and Z. Sadowski, *Physicochem. Probl. Miner. Process.*, 2017, **53**, 869–877.

36 O. A. Desouky, A. A. El-Moughith, W. A. Hassanien, G. S. Awadalla and S. S. Hussien, *Arabian J. Chem.*, 2016, **9**, S795–S805.

37 A. Kumari, M. K. Jha, K. Yoo, R. Panda, J. Y. Lee, J. R. Kumar and D. D. Pathak, *Hydrometallurgy*, 2019, **187**, 203–211.

38 Z. Han, J. Wang, H. Zhao, M. E. Tucker, Y. Zhao, G. Wu, J. Zhou, J. Yin, H. Zhang, X. Zhang and H. Yan, *Minerals*, 2019, **9**, 218.

39 K. C. Vinoth Kumar, T. Jani Subha, K. G. Ahila, B. Ravindran, S. W. Chang, A. H. Mahmoud, O. B. Mohammed and M. A. Rathi, *Saudi J. Biol. Sci.*, 2021, **28**, 840–846.

40 C. Kamaraj, S. Lakshmi, C. Rose and C. Muralidharan, *Asian J. Res. Soc. Sci. Humanit.*, 2017, **7**, 240.

41 H. Böke, S. Akkurt, S. Özdemir, E. H. Göktürk and E. N. Caner Saltik, *Mater. Lett.*, 2004, **58**, 723–726.

42 M. Marković, A. Daković, G. E. Rottinghaus, M. Kragović, A. Petković, D. Krajišnik, J. Milić, M. Mercurio and B. de Gennaro, *Colloids Surf., B*, 2017, **151**, 324–332.

43 I. V. Chernyshova, K. Hanumantha Rao, A. Vidyadhar and A. V. Shchukarev, *Langmuir*, 2000, **16**, 8071–8084.

44 X. Feng, Z. Long, D. Cui, L. Wang, X. Huang and G. Zhang, *Trans. Nonferrous Met. Soc. China*, 2013, **23**, 849–854.

45 Z. Ruan, M. Li, K. Gao, D. Zhang, L. Huang, W. Xu and X. Liu, *ACS Omega*, 2019, **4**, 9813–9822.

46 H. Fathollahzadeh, J. J. Eksteen, A. H. Kaksonen and E. L. J. Watkin, *Appl. Microbiol. Biotechnol.*, 2019, **103**, 1043–1057.

47 M. H. Derkani, A. J. Fletcher, M. Fedorov, W. Abdallah, B. Sauerer, J. Anderson and Z. J. Zhang, *Colloids Interfaces*, 2019, **3**, 62.

48 J. D. Chang, E. E. Vaughan, C. G. Liu, J. W. Jelinski, A. L. Terwilliger and A. W. Maresso, *Sci. Rep.*, 2021, **11**, 23917.

49 L. Perez-Fons, P. M. Bramley and P. D. Fraser, *Metabolomics*, 2014, **10**, 77–90.

